Chemical Science

ROYAL SOCIETY OF CHEMISTRY

EDGE ARTICLE

View Article Online
View Journal | View Issue

Cite this: *Chem. Sci.*, 2022, **13**, 11672

All publication charges for this article have been paid for by the Royal Society of Chemistry

Expanding new chemistry of aza-boracyclophanes with unique dipolar structures, AIE and redox-active open-shell characteristics†

Yawei Jia,[a] Pengfei Li,[a] Kanglei Liu,*[a] Chenglong Li,[a] Meiyan Liu,[a] Jiaqi Di,[a] Nan Wang,[a] Xiaodong Yin,[a] Niu Zhang*[b] and Pangkuan Chen*[a]

π-Conjugated macrocycles involving electron-deficient boron species have received increasing attention due to their intriguing tunable optoelectronic properties. However, most of the reported B(sp^2)-doped macrocycles are difficult to modify due to the synthetic challenge, which limits their further applications. Motivated by the research of non-strained hexameric bora- and aza-cyclophanes, we describe a new class of analogues **MC-BN5** and **MC-ABN5** that contain charge-reversed triarylborane (Ar_3B) units and oligomeric triarylamines (Ar_3N) in the cyclics. As predicted by DFT computations, the unique orientation of the donor–acceptor systems leads to an increased dipole moment compared with highly symmetric macrocycles (**M1**, **M2** and **M3**), which was experimentally represented by a significant solvatochromic effect with large Stokes shifts up to 12 318 cm^{-1}. Such a ring-structured design also allows the easy peripheral modification of aza-boracyclophanes with tetraphenylethenyl (TPE) groups, giving rise to a change in the luminescence mechanism from aggregation-caused quenching (ACQ) in **MC-BN5** to aggregation-induced emission (AIE) in **MC-ABN5**. The open-shell characteristics have been chemically enabled and were characterized by UV-Vis-NIR spectroscopy and electron paramagnetic resonance (EPR) for **MC-BN5**. The present study not only showed new electronic properties, but also could expand the research of B/N doped macrocycles into the future scope of supramolecular chemistry, as demonstrated in the accessible functionalization of ring systems.

Received 27th June 2022
Accepted 21st September 2022

DOI: 10.1039/d2sc03581b

rsc.li/chemical-science

Introduction

Macrocyclic structures have received much attention over the past two decades as they played a crucial role in host–guest chemistry,[1] organic light-emitting diodes (OLEDs),[2] biological science[3] and supramolecular assembly.[4] Macrocycles of π-electron systems exhibit particularly intriguing optical, electronic and magnetic behaviors owing to an equivalent of these cycles to well-defined open-chain polymers but with an infinite conjugation length.[2b,5] The incorporation of main group heteroatoms (such as B, N, and S) has proved an efficient strategy to build π-conjugated materials with unique optoelectronic properties.[6] Such a group of heteroatom-doped macrocycles are expected to show distinct electronic structures compared with all-carbon based analogues, and their frontier molecular orbitals can be tuned.

Ito and Tanaka *et al.* first reported a cyclic hexamer of an electron-rich arylamine macrocycle **M1**,[6g] and then some other macrocyclic oligoarylamines were also investigated.[6k,7] The electron-deficient triarylboron exhibits a remarkable electronic polarization and intramolecular charge transfer (ICT) in the presence of electron donors, leading to tunable emissions, enhanced charge-transport characteristics and unusual redox properties.[8] The Jäkle group pioneered boracyclophane chemistry by developing a fluoreneborane cycle (**MC-B6-Flu**),[6a] followed by an ambipolar macrocycle **M2** with alternating arylamines and arylboranes.[6b] They have recently designed a considerably electron-deficient **M3** with a low-lying LUMO and strong electronic affinity regardless of the synthetic challenge associated with the enhanced electron deficiency.[6d] In fact, all the above-represented macrocycles exhibit a dipole moment $\mu = 0$ in the ground state due to the highly symmetric geometry. Our group and coworkers proposed a new concept of a block-type macrocycle (**M4**) in which the electron-donor block (N3) and acceptor block (B3) are oriented on opposite sides (Scheme 1), leading to an increased dipole moment (μ_g) and a reduced HOMO–LUMO energy gap (E_{gap}).[9] Computations reveal that the

[a]*Beijing Key Laboratory of Photoelectronic/Electrophotonic Conversion Materials, Key Laboratory of Cluster Science of the Ministry of Education, Key Laboratory of Medical Molecule Science and Pharmaceutics Engineering of the Ministry of Industry and Information Technology, School of Chemistry and Chemical Engineering, Beijing Institute of Technology of China, Beijing, 102488, China. E-mail: kanglei_liu@bit.edu.cn; pangkuan@bit.edu.cn*

[b]*Analysis & Testing Centre, Beijing Institute of Technology of China, Beijing, 102488, China. E-mail: niuzhang2019@bit.edu.cn*

† Electronic supplementary information (ESI) available: Details of synthesis and characterization, DFT and TD-DFT calculations and others. See https://doi.org/10.1039/d2sc03581b

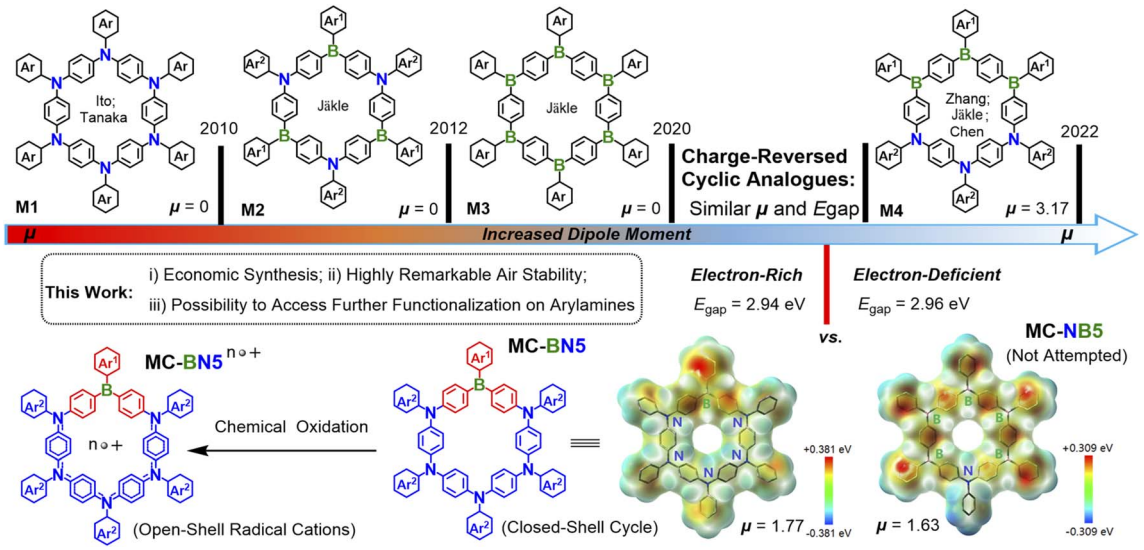

Scheme 1 Research foundation and design principle for the dipolar aza-boracyclophane **MC-BN5** in comparison to some of the π-conjugated systems of B/N-doped cyclic hexamers **M1**, **M2**, **M3** and **M4**.

specific patterns of B and N centers as well as the molecular symmetry are closely related to the μ_g and E_{gap} levels (Fig. S28†), which dramatically impact the respective photophysical and electronic properties.

To further expand the research scope of boracyclophane chemistry, we turned our attention to B/N doped macrocycles in low symmetry with accessible functionalized peripheries. In this respect, we conceive two model cycles **MC-BN5** and **MC-NB5** that are charge-reversed analogues and show similar dipole moments and energy gaps (**MC-BN5:** $\mu_g = 1.77$ and $E_{gap} = 2.94$ eV; **MC-NB5:** $\mu_g = 1.63$ and $E_{gap} = 2.96$ eV). However, the stepwise synthesis of pentameric triarylboranes seems to require steric shielding for the latter under strictly inert conditions given a gradually increased number of borons as Lewis acid sites. In contrast, oligotriarylamines can be readily accessible for the former cycle using some more step-economic reactions *via* transition-metal-catalyzed C–N cross-couplings. For future generations of aza-boracyclophanes, the donor segments of oligoarylamines selected with a high tolerance to air are of particular significance, as they allow further manipulation and processes to be reasonably achieved. Accordingly, we herein describe an efficient design strategy toward **MC-BN5** and the derivative **MC-ABN5**. **MC-BN5** strongly red-shifted the emission to orange in polar solvents from the green color for analogous boracyclophanes (**M2**, **M3** and **MC-B6-Flu**), and the open-shell radical species enabled by chemical oxidation were also monitored by UV-Vis-NIR spectroscopy and electron paramagnetic resonance (EPR) spectroscopy. More importantly, peripheral substitutions of tetraphenylethyl (TPE) units at the π-ring structure of **MC-ABN5** with radial p orbitals induced a transformation of aggregation-caused quenching (ACQ) to a rarely observed aggregation-induced emission (AIE) for π-conjugated macrocycles.[4b,6n,10] Our strategy may provide a new possibility to develop directions in supramolecular chemistry using highly stable dipolar macrocycles.

Results and discussion

The synthetic routes and data toward **MC-BN5** and **MC-ABN5** are depicted in Scheme 2 and the ESI.† Precursor **1** was obtained through the gradual build-up of oligomerization according to previously reported procedures.[9] Starting from the dihalogenated arylamine trimer **1**, π-extended pentamers **2** and **3** were prepared by Buchwald–Hartwig coupling with 4-hexylaniline and 4-tetraphenylethenyl amine (TPE-NH_2), respectively. Similar reactions in the subsequent C–N cross-couplings yielded the key intermediates **4** and **5**. The lithiation of dibrominated **4** and **5** followed by the addition of $TipB(OMe)_2$ as a protected boron source was performed in dilute ether solutions to stitch the π-extended oligoarylamines, and it resulted in aza-boracyclophanes **MC-BN5** in 30% and **MC-ABN5** in 15% isolated yields.

Both macrocycles are stable enough in air and can be easily purified by column chromatography on silica gel without particular precautions. The structures of **MC-BN5** and **MC-ABN5** were fully characterized by multinuclear NMR and high-resolution mass spectroscopy (ESI†). MALDI-TOF-MS spectra clearly showed a single peak (Scheme 2b, Fig. S8 and S16†), corresponding to the molecular-ion peak at $m/z = 1462.9664$ for **MC-BN5** (calcd 1462.9673) and at 1802.9986 for **MC-ABN5** (calcd 1802.9988). The broad bands centered at 31 and 56 ppm in the ^{11}B NMR spectra for **MC-BN5** **MC-ABN5**, respectively, confirmed the incorporation of tricoordinate arylborane species (Fig. S7 and S15†). Notably, two of the macrocycles showed no visible changes in solution after storage over a few months at ambient temperature, indicating exceptionally high structural persistence which is somewhat superior to that of **M4** (Fig. S18†).

The photophysical properties of **MC-BN5** and **MC-ABN5** were explored by UV-Vis absorption and emission spectroscopy (Fig. 1 and ESI†). Both **MC-BN5** and **MC-ABN5** showed a strong absorption band at 347 and 364 nm in CH_2Cl_2, respectively,

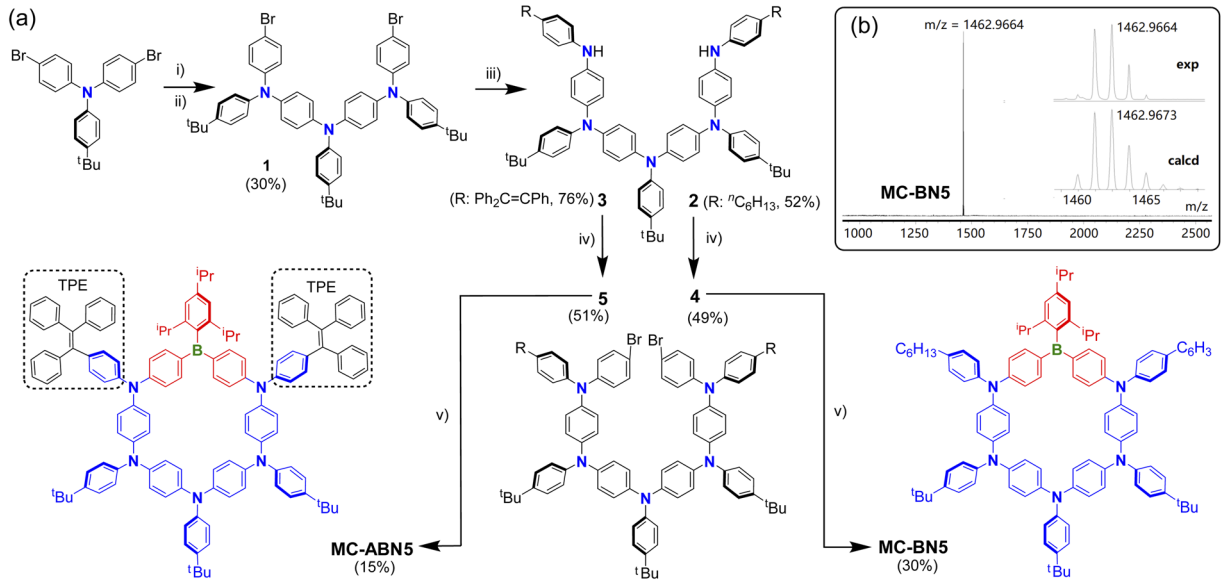

Scheme 2 (a) Key steps in the synthesis of **MC-BN5** and **MC-ABN5**. **1** was synthesized by similar procedures reported (see ref. 9). Reagents and conditions: (i) 4-^{t}Bu-aniline, Pd(dppf)Cl_2, DPPF, ^{t}BuONa, toluene, and reflux. (ii) *para*-Bromo-iodobenzene, Pd(dppf)Cl_2, DPPF, ^{t}BuONa, toluene, and reflux. (iii) Pd(dppf)Cl_2, DPPF, ^{t}BuONa, 4-^{n}hexyl-aniline (for **2**) or 4-tetraphenylethenyl amine (TPE-NH_2, for **3**), toluene, and reflux. (v) ^{n}BuLi, TipB(OMe)$_2$, ether, and −35 °C to reflux overnight. Tip = 2,4,6-triisopropylphenyl. (b) MAIDI-TOF-MS (positive-ion mode) of **MC-BN5** showing experimental and simulated isotopic patterns.

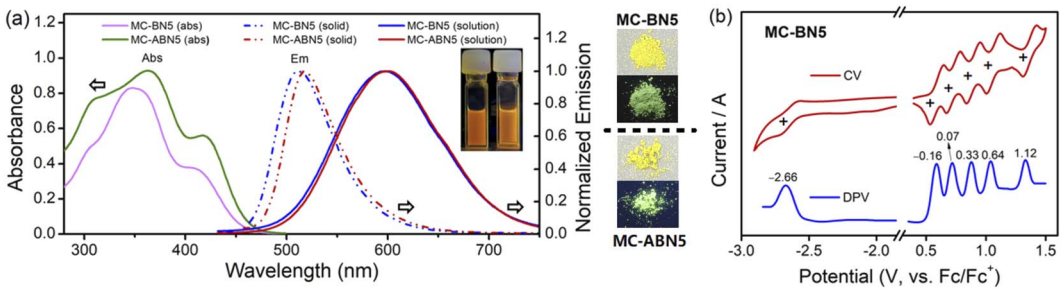

Fig. 1 (a) UV-Vis absorption and emission spectrum of **MC-BN5** (λ_{ex} = 408 nm) and **MC-ABN5** (λ_{ex} = 417 nm) both in CH_2Cl_2 ($c = 1 \times 10^{-5}$ M) and in the solid state. Inset: photographs of solutions **MC-BN5** and **MC-ABN5** and respective solids under ambient light (upper) and 365 nm UV irradiation (down). (b) Cyclic and differential pulse voltammetry (CV and DPV) curves (*vs.* Fc^+/Fc) in CH_2Cl_2 (oxidative potential) and THF (reductive potential), using *n*-Bu_4NPF_6 (0.1 M) as the electrolyte, and v = 100 mV s^{-1}.

which were assigned to π–π* transitions (Fig. 1a). Meanwhile, they also displayed a low-energy shoulder peak at 408 (**MC-BN5**) and 417 nm (**MC-ABN5**), respectively, ascribed to an intramolecular charge transfer (ICT) from the electron-donating moieties (–N–π–N–π–N–π–N–π–N–) to the electron-accepting unit (–π–B–π–). Two molecules show similar absorption profiles but with slightly red-shifted bands for **MC-ABN5**, as a result of the extended π-conjugation effect by TPE substituents at the six-membered periphery of **MC-BN5**. The optical energy gap $E_{gap(optical)}$ was determined to be 2.70 eV for **MC-BN5**, consistent with the computed results ($E_{gap(DFT)}$: 3.02 eV; $E_{gap(TDDFT)}$: 2.73 eV, Table 1 and ESI†).

MC-BN5 and **MC-ABN5** emitted orange fluorescence in CH_2Cl_2 (**MC-BN5:** λ_{em} = 597 nm and Φ_F = 16%; **MC-ABN5:** λ_{em} = 600 nm and Φ_F = 10%), which is significantly red-shifted from analogous boracyclophanes involving **M2**,[6b] **M3** (ref. 6*d*) and **MC-B6-Flu**.[6a] They showed green color emissions in the solid state (**MC-BN5:** 512 nm and Φ_F = 13%; **MC-ABN5:** 517 nm and Φ_F = 37%), and the emission quantum efficiency of **MC-BN5** was reduced relative to that in solution, in line with a traditional ACQ mechanism. However, the blue-shifted emission of **MC-ABN5** was enhanced as solids and was in accordance with AIE activity due to the TPE incorporation. As shown in the solvatochromic emissions, **MC-BN5** and **MC-ABN5** change their colors from blue-sky in hexane (λ_{em}: ~490 nm) to orange in highly polar solvents (λ_{em}: ~600 nm) with large Stokes shifts up to 12 318 and 10 806 cm^{-1}, respectively (Fig. 2a and ESI†). Large slopes of the data fitting in Lippert–Mataga plots further denote an apparent ICT character that is an indication of much more polar structures in **MC-BN5** and **MC-ABN5** than other highly symmetric boracyclophanes such as **M2**, **M3**, **MC-B6-Flu**, **MC-B4N2**[6c] and **MC-B4N2-^{F}Mes**[6e] (Fig. 2b and Table S4†).

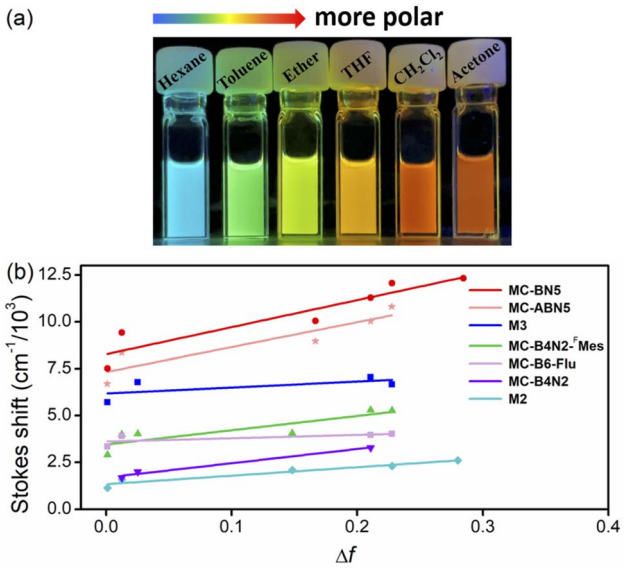

Fig. 2 (a) Photographs of **MC-BN5** in solvents of different polarity upon irritation at 365 nm (left to right: *n*-hexane, toluene, ether, THF, CH_2Cl_2 and acetone). (b) Lippert–Mataga plots for solvatochromic emissions of **MC-BN5** and **MC-ABN5** in comparison to some other representative B-containing macrocycles.

The electrochemical properties of **MC-BN5** were examined by cyclic (CV) and differential pulse voltammetry (DPV) (Fig. 1b). **MC-BN5** showed five fully reversible 1e oxidation bands with the first half-wave potential at $E_{1/2}^{ox} = -0.16$ V (*vs.* Fc/Fc^+, CH_2Cl_2) and a reversible reduction band at $E_{1/2}^{red} = -2.66$ V (*vs.* Fc/Fc^+, THF). These well-separated patterns are attributed to the sequential oxidations at each of the Ar_3N moieties with strong electronic couplings. The six-membered aza/boracyclophane analogues show a trend of the oxidations toward higher potentials with a decreased number of arylamines: **M1** (−0.28 V, N6) < **MC-BN5** (−0.16 V, N5) < **M4** (+0.02 V, *b*-N3) < **M2** (+0.46 V, *alt*-N3), in line with the trend of reduced HOMO energy levels. A similar observation is also the case in the reductions with increasing B centers: **MC-BN5** (−2.66 V, B1) < **M2** (−2.53 V, *alt*-B3) < **M4** (−2.10 V, *b*-B3) < **M3** (−1.56 V, B6) and agrees very well with the trend of the computed LUMO energies (Table S5†). These results suggest that the number as well as the orientation of B and/or N arranged in macrocyclic architectures could effectively impact the electronic structures and molecular symmetry. **MC-BN5** shows a smaller electrochemical energy gap ($E_{gap(elec)} = 2.50$ eV) than the linear **L-B_2N_5** ($E_{gap(elec)} = 2.61$ eV) that involves five units of oligomeric arylamines end-capped by the two terminal arylboranes, leading to a higher oxidation potential ($E^{ox1} = 0.01$ V) in the open-chain structure.[13c]

MC-BN5 exhibits a more polar structure compared with the highly symmetric aza-boracyclophanes, which can be confirmed by a stronger dipole moment ($\mu_g = 1.77$ D) than that of 0 D calculated for the simplified analogues **M2** and **M3** (*i.e.*, alternating ambipolar MC-*alt*-B3N3 in D_3 and electron-deficient MC-B6 in D_{3d}, and $\mu_g = 0$ D). According to computational results, **MC-BN5** should be slightly less polar than the cyclic hexamer **M4** (block-type MC-*b*-B3N3: C_2, and $\mu_g = 3.17$ D), but closely resembles the charge-reversed model compound **MC-NB5** with $\mu_g = 1.63$ D in a similar C_2 symmetry (Fig. S28†). As visualized in the electrostatic potential (ESP) map, **MC-BN5** shows an electronic structure with electron-donating triarylamines negatively charged and the borane acceptor observed in the positive domain (Scheme 1).

The electronic structure of simplified **MC-BN5** was further elucidated by DFT (B3LYP, 6-31G*) and TD-DFT (B3LYP/CAM-B3LYP, 6-311G*) calculations (Fig. 3 and ESI†). The highest occupied molecular orbital (HOMO) is delocalized over the electron-rich pentatriarylamine block (N5), whereas the lowest unoccupied molecular orbital (LUMO) is only located B-centered with a small contribution from the adjacent N atoms. HOMO−1 and HOMO−2 are both delocalized nearly in the ring skeleton. TD-DFT reveals the lowest energy transition to S_1 ($f = 0.1600$) due to charge transfer from the Ar_3N to the Ar_3B moiety, which however was usually symmetry-forbidden in highly symmetric cyclic structures including **M1**, **M2**, **M3** and others.[6a,c,e] Such a dissymmetry-allowed HOMO–LUMO transition was also the case for the block-type macrocycle **M4** with a lower symmetry.[9] Vertical excitations to higher energy states up to S_5 are attributed to a mixed pathway involving the π–π* transition of phenyl linkers and charge transfers from triarylamine moieties (*i.e.* endocyclic phenyl or exocyclic aryl) to endocyclic arylborane, and the n–π* transitions from N sites also contribute.

As seen in the above-mentioned electrochemical characterization, **MC-BN5** exhibits fully reversible oxidation events due to sequential oxidations of all the five arylamines to radical cation species. A chemical oxidation approach for **MC-BN5** using $AgSbF_6$ was also performed to investigate its cationic states under strictly inert conditions, and *in situ* UV-Vis-NIR

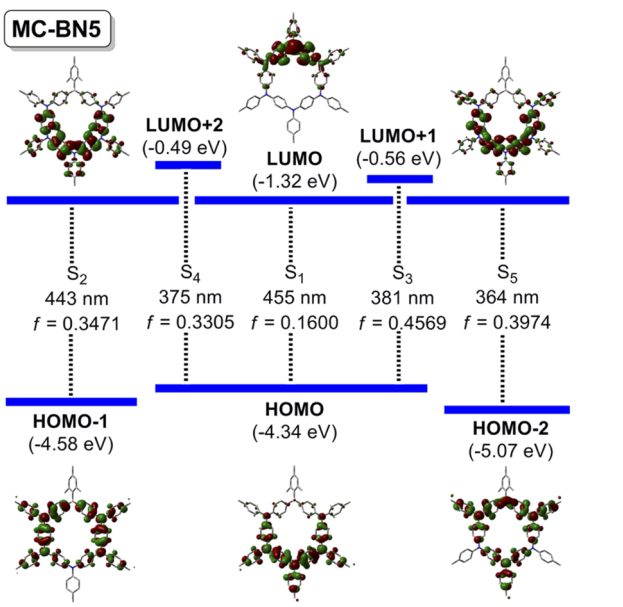

Fig. 3 Key electronic transitions contributing to vertical excitations of simplified **MC-BN5** (TD-DFT, B3LYP/6-311G*) with molecular orbital plots (iso = 0.02, B3LYP/6-31G*). The ^{i}Pr, ^{t}Bu and ^{n}Hex groups are simplified as methyl groups.

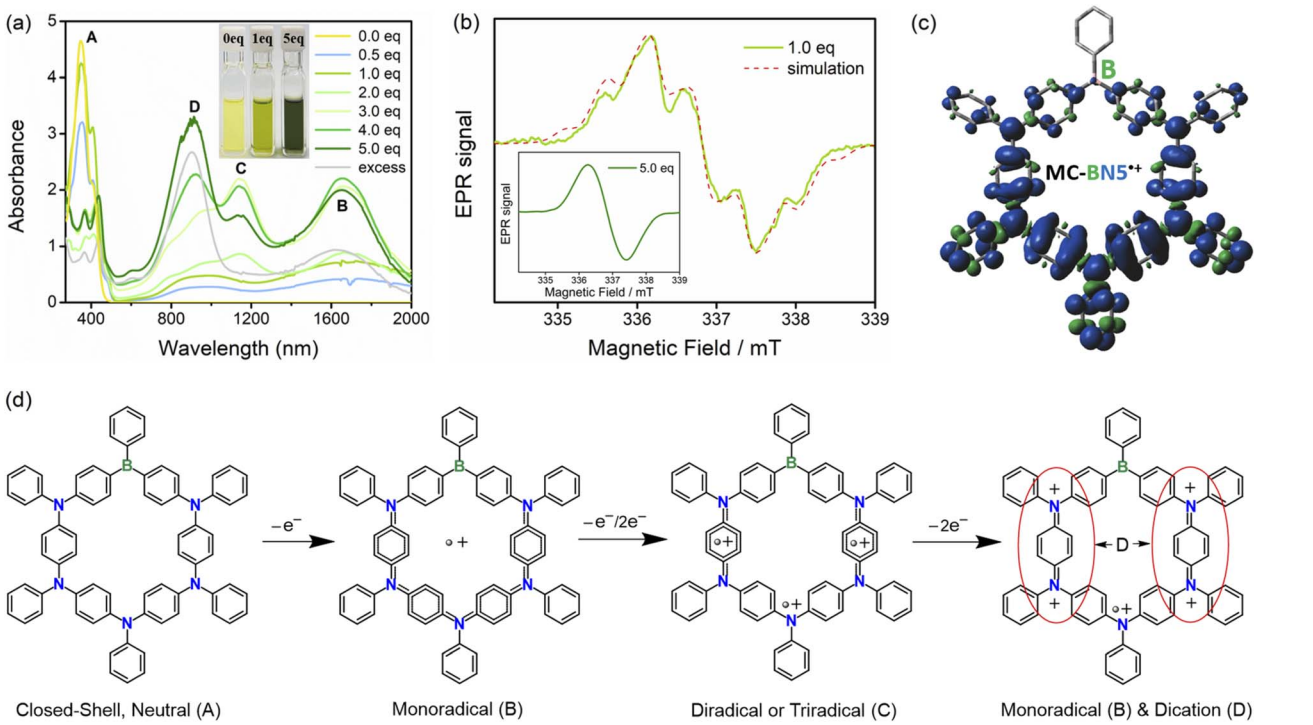

Fig. 4 (a) Chemical oxidations of **MC-BN5** ($c = 5.0 \times 10^{-5}$ M) monitored by UV-Vis-NIR absorption spectroscopy with different amounts of $AgSbF_6$. Inset: photographs of **MC-BN5** solutions with 0.0, 1.0 and 5.0 equiv. of $AgSbF_6$. The EPR spectra of **MC-BN5** ($c = 2.0 \times 10^{-4}$ M in CH_2Cl_2 under N_2): (b) 1.0 equiv. of $AgSbF_6$ (solid line) and simulation (dashed line). Inset: 5.0 equiv. of $AgSbF_6$. (c) Spin density distribution of the monoradical **MC-BN5**$^{\bullet+}$ (UB3LYP/6-31G(d,p); blue: positive spin and green: negative spin). (d) Schematic assignments of the oxidized species of **MC-BN5** with the addition of $AgSbF_6$. Substituents on arylboranes and arylamines are simplified as H atoms for clarity.

spectroscopy and electron paramagnetic resonance (EPR) were conducted.[6o] As shown in Fig. 4a, the addition of an approximately stoichiometric amount of $AgSbF_6$ to **MC-BN5** solution in CH_2Cl_2 provided a green-colored reaction mixture at room temperature. Compared with the neutral **MC-BN5** (A), the oxidized species displayed two new broad absorption bands at *ca.* 900 and 1650 nm, and the latter band at a longer wavelength should be ascribed to the formation of the monoradical cation **MC-BN5**$^{\bullet+}$ (B, Fig. 4d). This UV-Vis-NIR spectrum response to oxidation assigned to the spin-delocalized open-shell species can be confirmed by a split EPR spectrum with a ^{14}N-hyperfine coupling constant $\alpha(^{14}N) = 0.826$ mT, $\alpha(^{1}H) = 1.424$ mT and $g = 2.0037$ (Fig. 4b and c).[6g]

Oxidation titration by further addition of $AgSbF_6$ up to 5 equiv. led to a significantly increased intensity of the long wavelength band and also to a new NIR absorption peak at *ca.* 1150 nm, corresponding to the generation of higher oxidation states including radical dications and/or trications (C). Upon increasing the amount of $AgSbF_6$, this new absorption band gradually disappeared, while both signals of the intense higher-energy and lower-energy bands ($\lambda_{abs} = 900$ and 1650 nm) were maintained even in the presence of an excess of $AgSbF_6$. These observations are in agreement with the speculation that monoradicals (B) are initially formed along with a small number of diamagnetic quinoidal dications (D) and that the reaction solution can be gradually dominated by the resulting spinless dication species.[7,11] The fully oxidized **MC-BN5** was proved very stable in air (Fig. S26†) and showed a featureless broad signal with a *g*-value of 2.0037 in the EPR spectrum (Fig. 4b, inset), indicating the absence of spin–spin dipole interactions due to a higher degree of the oxidation processes.

MC-BN5 showed a reduced emission in toluene with increased concentrations, in accordance with the commonly found aggregation-caused quenching (ACQ) behavior (Fig. 5a). However, its macrocyclic derivative **MC-ABN5** showed in the solid state an enhanced emission quantum efficiency ($\Phi_S = 0.37$) relative to that of $\Phi_L = 0.10$ in solution (Table 1). These differences in the emissions are significant to indicate the unique electronic properties of B/N macrocycles. As shown in Fig. 5c, **MC-ABN5** maintained relatively low fluorescence profiles up to $f_{MeOH} = 70\%$ of the solvent mixture CH_2Cl_2/MeOH. Further increases in MeOH fractions gave rise to a dramatically enhanced emission intensity of **MC-ABN5** with a marked blue-shift of the emission bands from the orange emission (*ca.* 600 nm) to a bright green emission (*ca.* 535 nm) as well as an increased quantum yield up to $\Phi_F = 0.43$ with the emission lifetimes on the order of nanoseconds (Fig. S20a, Table S6†). This observation in agreement with the well-known aggregation-induced emission (AIE) mechanism supported by the dynamic light scattering (DLS) data (Fig. S20b†) is the consequence of structural functionalization with tetraphenylethyl (TPE) groups.[10,12] To the best of our knowledge, tricoordinated organoboranes including boron-based macrocycles have rarely been reported to show AIE properties.[13] Our

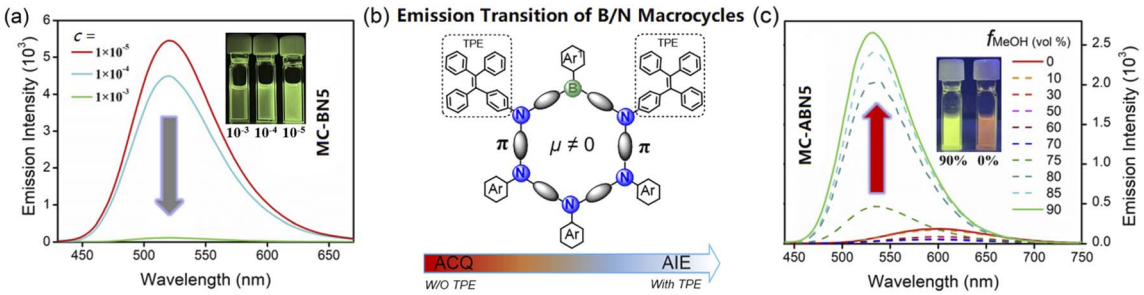

Fig. 5 TPE-enabled emission transition of B/N macrocycles from ACQ in **MC-BN5** (a) to the AIE mechanism in **MC-ABN5** (b, c): fluorescence spectra recorded in CH_2Cl_2/MeOH with increasing MeOH fractions f_{MeOH} ($c = 1.0 \times 10^{-5}$ M and $\lambda_{ex} = 408$ nm). Inset: photographs under 365 nm UV light.

Table 1 Summary of the photophysical, computational and electrochemical data

Compound	λ_{abs}[a] (nm)	λ_{em}[a] (nm)	λ_{em}[b] (nm)	Φ_L[c] (%)	Φ_S[d] (%)	τ_{av}[e] (ns)	$E_{HOMO}/E_{LUMO}/E_{gap(DFT)}$[f] (eV)/(eV)	E_{TDDFT}[g] (eV)	$E_{gap(optical)}$[h] (eV)	$E^{ox1}/E^{red1}/E_{gap(elec)}$[i] (V)/(eV)
MC-BN5	347, 408	597	512	16	13	4	−4.34/−1.32/3.02	2.73	2.70	−0.16/−2.66/2.50
MC-ABN5	364, 417	600	517	10	37	3	—	—	2.63	—

[a] Recorded in CH_2Cl_2 ($c = 1.0 \times 10^{-5}$ M). [b] Emission in the solid state. [c] Emission quantum efficiency (Φ_L) in CH_2Cl_2. [d] Emission quantum efficiency (Φ_S) in the solid state. [e] Emission lifetime (τ_{av}) in CH_2Cl_2. [f] Energy gap: $E_{gap} = E_{LUMO} - E_{HOMO}$ obtained by DFT calculation (B3LYP, 6-31G*). [g] Vertical excitation of the lowest energy transition ($S_0 \rightarrow S_1$) calculated by TD-DFT (B3LYP, 6-311G*). [h] $E_{gap(optical)}$: optical energy gap experimentally obtained from the onsets of the lowest energy absorption band in toluene. [i] Electrochemical energy gap determined by the first peak potential of oxidation (E^{ox1}) and reduction (E^{red1}) in differential pulse voltammetry (*vs.* Fc^+/Fc).

molecular design for the optically reversed emission transition from ACQ to AIE represented by **MC-BN5** and **MC-ABN5** affords a new approach to aggregated macrocyclic chemistry, and it may also provide a proof of concept for supramolecular assembly using polar-structured π-conjugated cyclics.

MC-BN5 and **MC-ABN5** are also of interest as responsive materials. First, we have monitored the variable-temperature (VT) emission spectra in 2-methyltetrahydrofuran (Fig. S21†). With the temperature gradually increased, **MC-BN5** was blue-shifted by *ca.* 60 nm in the emission from $\lambda_{em} = 625$ nm at 140 K to 567 nm at 340 K. This thermochromic response was fully reversible and displayed an excellent fatigue resistance without emission degradation when exposed to 5 cycles of alternating temperature. A similar behavior was also observed for **MC-ABN5** but with a slightly stronger bathochromic shift of 70 nm. Second, given the presence of electron-deficient organoborane moieties, we performed anion binding studies of **MC-BN5** with tetrabutylammonium fluoride (TBAF) in THF. **MC-BN5** showed a gradual decrease of the typical charge-transfer absorption band at 408 nm, along with a gradual emission quenching in response to the titration of F^- (Fig. S22†).

Conclusions

We report an efficient synthetic strategy to access new B/N doped macrocycles **MC-BN5** and **MC-ABN5** by structural stitching of electron-donating oligoarylamine pentamers using arylborane donor segments, leading to electronically unique low-symmetry aza-boracyclophanes ($\mu_g = 1.77$ in **MC-BN5**). They displayed considerably stronger charge transfer properties and reduced HOMO–LUMO energy gaps in comparison to those established highly symmetric aza/boracyclophane analogues with a dipole moment $\mu_g = 0$. These results suggest that the number ratio of B/N as well as their orientations can be readily tuned in macrocyclic architectures, which are essential to understand the impact of electronic structures and molecular symmetry on their optoelectronic characteristics. Beyond these findings, the environmental susceptibility of dipolar cycles was sufficiently counterbalanced to achieve exceptionally high stability that allowed chemically oxidation-induced open-shell radical species in **MC-BN5** and aggregation-induced emission of its derivative **MC-ABN5** under ambient conditions. We envision that the molecular derivatization of **MC-BN5** is targeted not only for the emission transition between ACQ and AIE, but is truly approaching new directions in the supramolecular chemistry of polar-structured conjugated macrocycles. Pursuit for further studies on supramolecular systems related to this concept is ongoing in our laboratory.

Data availability

All data supporting this study are included in the paper and provided in the ESI† accompanying this paper at the journal's website.

Author contributions

Y. J., P. L. and P. C. conceived the project. Y. J. carried out all the synthetic experiments and analysed the experimental data. Y. J., P. L. and K. L. drafted the manuscript and revised the

manuscript. P. L., C. L. and Y. J. performed the electrochemical measurements. M. L. obtained the solid quantum efficiency data. C. L. and J. D. acquired the MALDI-TOF-MS data. N. W. and X. Y. gave suggestions on the work. N. Z. provided help with mass spectroscopy and AIE measurements and also contributed to the write-up of the main manuscript. P. C. was responsible for the guidance of this project and finalized the manuscript as well as all calculations.

Conflicts of interest

There are no conflicts to declare.

Acknowledgements

This work was supported by the National Natural Science Foundation of China (NSFC) (No. 21772012 and 22101025). We are greatly thankful to Prof. Suning Wang at Queen's University for helpful discussions over the years. We thank the Analysis & Testing Center at the Beijing Institute of Technology for advanced facilities. The authors acknowledge the Analysis Center, Department of Chemistry at Tsinghua University for EPR experiments.

Notes and references

1 (*a*) T. Kawase and H. Kurata, *Chem. Rev.*, 2006, **106**, 5250–5273; (*b*) M. Iyoda, J. Yamakawa and M. J. Rahman, *Angew. Chem., Int. Ed.*, 2011, **50**, 10522–10553; (*c*) M.-X. Wang, *Acc. Chem. Res.*, 2012, **45**, 182–195; (*d*) Z. Liu, S. K. M. Nalluri and J. F. Stoddart, *Chem. Soc. Rev.*, 2017, **46**, 2459–2478; (*e*) J. E. M. Lewis, P. D. Beer, S. J. Loeb and S. M. Goldup, *Chem. Soc. Rev.*, 2017, **46**, 2577–2591; (*f*) C.-F. Chen and Y. Han, *Acc. Chem. Res.*, 2018, **51**, 2093–2106; (*g*) X. Ji, M. Ahmed, L. Long, N. M. Khashab, F. Huang and J. L. Sessler, *Chem. Rev.*, 2019, **48**, 2682–2697; (*h*) D. Xia, P. Wang, X. Ji, N. M. Khashab, J. L. Sessler and F. Huang, *Chem. Rev.*, 2020, **120**, 6070–6123; (*i*) S. V. Bhosale, M. A. Kobaisi, R. W. Jadhav, P. P. Morajkar, L. A. Jones and S. George, *Chem. Soc. Rev.*, 2021, **50**, 9845–9998; (*j*) H. Nie, Z. Wei, X.-L. Ni and Y. Liu, *Chem. Rev.*, 2022, **122**, 9032–9077.

2 (*a*) J. Y. Xue, T. Izumi, A. Yoshii, K. Ikemoto, T. Koretsune, R. Akashi, R. Arita, H. Taka, H. Kita, S. Sato and H. Isobe, *Chem. Sci.*, 2016, **7**, 896–904; (*b*) S. Izumi, H. F. Higginbotham, A. Nyga, P. Stachelek, N. Tohnai, P. Silva, P. Data, Y. Takeda and S. Minakata, *J. Am. Chem. Soc.*, 2020, **142**, 1482–1491.

3 (*a*) A. K. Yudin, *Chem. Sci.*, 2015, **6**, 30–49; (*b*) R. Pinalli, A. Pedrini and E. Dalcanale, *Chem. Soc. Rev.*, 2018, **47**, 7006–7026; (*c*) N. Song, Z. Zhang, P. Liu, Y.-W. Yang, L. Wang, D. Wang and B. Z. Tang, *Adv. Mater.*, 2020, **32**, 2004208; (*d*) Y. Qin, X. Liu, P.-P. Jia, L. Xu and H.-B. Yang, *Chem. Soc. Rev.*, 2020, **49**, 5678–5703.

4 (*a*) R. Chakrabarty, P. S. Mukherjee and P. J. Stang, *Chem. Rev.*, 2011, **111**, 6810–6918; (*b*) S.-N. Lei, H. Xiao, Y. Zeng, C.-H. Tung, L.-Z. Wu and H. Cong, *Angew. Chem., Int. Ed.*, 2020, **59**, 10059–10065; (*c*) F. Picini, S. Schneider, O. Gavat, A. V. Jentzsch, J. Tan, M. Maaloum, J.-M. Strub, S. Tokunaga, J.-M. Lehn, E. Moulin and N. Giuseppone, *J. Am. Chem. Soc.*, 2021, **143**, 6498–6504; (*d*) S. Kawano, M. Nakaya, M. Saitow, A. Ishiguro, T. Yanai, J. Onoe and K. Tanaka, *J. Am. Chem. Soc.*, 2022, **144**, 6749–6758.

5 (*a*) Q.-H. Guo, Y. Qiu, M.-X. Wang and J. F. Stoddart, *Nat. Chem.*, 2021, **13**, 402–419; (*b*) T. A. Schaub, E. A. Prantl, J. Kohn, M. Bursch, C. R. Marshall, E. J. Leonhardt, T. C. Lovell, L. N. Zakharov, C. K. Brozek, S. R. Waldvogel, S. Grimme and R. Jasti, *J. Am. Chem. Soc.*, 2020, **142**, 8763–8775; (*c*) H. Zhu, I. Badía-Domínguez, B. Shi, Q. Li, P. Wei, H. Xing, M. C. R. Delgado and F. Huang, *J. Am. Chem. Soc.*, 2021, **143**, 2164–2169; (*d*) W. Fan, T. Matsuno, Y. Han, X. Wang, Q. Zhou, H. Isobe and J. Wu, *J. Am. Chem. Soc.*, 2021, **143**, 15924–15929; (*e*) M. Krzeszewski, H. Ito and K. Itami, *J. Am. Chem. Soc.*, 2022, **144**, 862–871; (*f*) K. Li, Z. Xu, J. Xu, T. Weng, X. Chen, S. Sato, J. Wu and Z. Sun, *J. Am. Chem. Soc.*, 2021, **143**, 20419–20430.

6 (*a*) P. Chen and F. Jäkle, *J. Am. Chem. Soc.*, 2011, **133**, 20142–20145; (*b*) P. Chen, R. A. Lalancette and F. Jäkle, *Angew. Chem., Int. Ed.*, 2012, **51**, 7994–7998; (*c*) P. Chen, X. Yin, N. Baser-Kirazli and F. Jäkle, *Angew. Chem., Int. Ed.*, 2015, **54**, 10768–10772; (*d*) N. Baser-Kirazli, R. A. Lalancette and F. Jäkle, *Angew. Chem., Int. Ed.*, 2020, **59**, 8689–8697; (*e*) N. Baser-Kirazli, R. A. Lalancette and F. Jäkle, *Organometallics*, 2021, **40**, 520–528; (*f*) D. Shimoyama, N. Baser-Kirazli, R. A. Lalancette and F. Jäkle, *Angew. Chem., Int. Ed.*, 2021, **60**, 17942–17946; (*g*) A. Ito, Y. Yokoyama, R. Aihara, K. Fukui, S. Eguchi, K. Shizu, T. Sato and K. Tanaka, *Angew. Chem., Int. Ed.*, 2010, **49**, 8205–8208; (*h*) F. P. Gabbaï, *Angew. Chem., Int. Ed.*, 2012, **51**, 6316–6318; (*i*) X.-Y. Wang, F.-D. Zhuang, R.-B. Wang, X.-C. Wang, X.-Y. Cao, J.-Y. Wang and J. Pei, *J. Am. Chem. Soc.*, 2014, **136**, 3764–3767; (*j*) M. Iyoda and H. Shimizu, *Chem. Soc. Rev.*, 2015, **44**, 6411–6424; (*k*) A. Ito, *J. Mater. Chem. C*, 2016, **4**, 4614–4625; (*l*) M. Stępień, E. Gońka, M. Żyła and N. Sprutta, *Chem. Rev.*, 2017, **117**, 3479–3716; (*m*) M. Hirai, N. Tanaka, M. Sakai and S. Yamaguchi, *Chem. Rev.*, 2019, **119**, 8291–8331; (*n*) Y. Li, A. Yagi and K. Itami, *J. Am. Chem. Soc.*, 2020, **142**, 3246–3253; (*o*) H. Sato, R. Suizu, T. Kato, A. Yagi, Y. Segawa, K. Awaga and K. Itami, *Chem. Sci.*, 2022, **13**, 9947–9951.

7 (*a*) A. Ito, Y. Yamagishi, K. Fukui, S. Inoue, Y. Hirao, K. Furukawa, T. Kato and K. Tanaka, *Chem. Commun.*, 2008, 6573–6575; (*b*) I. Kulszewicz-Bajer, V. Maurel, S. Gambarelli, I. Wielgus and D. Djurado, *Phys. Chem. Chem. Phys.*, 2009, **11**, 1362–1368; (*c*) D. Sakamaki, A. Ito, K. Furukawa, T. Kato and K. Tanaka, *Chem. Commun.*, 2009, 4524–4526; (*d*) T.-F. Yang, K. Y. Chiu, H.-C. Cheng, Y. W. Lee, M. Y. Kuo and Y. O. Su, *J. Org. Chem.*, 2012, **77**, 8627–8633; (*e*) D. Sakamaki, A. Ito, Y. Tsutsui and S. Seki, *J. Org. Chem.*, 2017, **82**, 13348–13358; (*f*) L. Skorka, P. Kurzep, T. Chauviré, L. Dubois, J.-M. Mouesca, V. Maurel and I. Kulszewicz-Bajer, *J. Phys. Chem. B*, 2017, **121**, 4293–4298; (*g*) W. Wang, C. Chen, C. Shu, S. Rajca, X. Wang and A. Rajca, *J. Am. Chem. Soc.*, 2018, **140**, 7820–7826.

8 (*a*) F. Jäkle, *Chem. Rev.*, 2010, **110**, 3985–4022; (*b*) A. G. Bonn and O. S. Wenger, *J. Org. Chem.*, 2015, **80**, 4097–4107; (*c*) L. Ji, S. Griesbeck and T. B. Marder, *Chem. Sci.*, 2017, **8**, 846–863; (*d*) K. Liu, R. A. Lalancette and F. Jäkle, *J. Am. Chem. Soc.*, 2017, **139**, 18170–18173; (*e*) C. Li, Y. Liu, Z. Sun, J. Zhang, M. Liu, C. Zhang, Q. Zhang, H. Wang and X. Liu, *Org. Lett.*, 2018, **20**, 2806–2810; (*f*) S. K. Mellerup and S. Wang, *Chem. Soc. Rev.*, 2019, **48**, 3537–3549; (*g*) Z.-B. Sun, J.-K. Liu, D.-F. Yuan, Z.-H. Zhao, X.-Z. Zhu, D.-H. Liu, Q. Peng and C.-H. Zhao, *Angew. Chem., Int. Ed.*, 2019, **58**, 4840–4846; (*h*) Z. Huang, S. Wang, R. D. Dewhurst, N. V. Ignat'ev, M. Finze and H. Braunschweig, *Angew. Chem., Int. Ed.*, 2020, **59**, 8800–8816; (*i*) A. S. Scholz, J. G. Massoth, M. Bursch, J.-M. Mewes, T. Hetzke, B. Wolf, M. Bolte, H.-W. Lerner, S. Grimme and M. Wagner, *J. Am. Chem. Soc.*, 2020, **142**, 11072–11083; (*j*) Y. Fu, H. Yang, Y. Gao, L. Huang, R. Berger, J. Liu, H. Lu, Z. Cheng, S. Du, H.-J. Gao and X. Feng, *Angew. Chem., Int. Ed.*, 2020, **59**, 8873–8879; (*k*) B. Adelizzi, P. Chidchob, N. Tanaka, B. A. G. Lamers, S. C. J. Meskers, S. Ogi, A. R. A. Palmans, S. Yamaguchi and E. W. Meijer, *J. Am. Chem. Soc.*, 2020, **142**, 16681–16689; (*l*) X. Su, T. A. Bartholome, J. R. Tidwell, A. Pujol, S. Yruegas, J. J. Martinez and C. D. Martin, *Chem. Rev.*, 2021, **121**, 4147–4192; (*m*) P.-F. Zhang, J.-C. Zeng, F.-D. Zhuang, K.-X. Zhao, Z.-H. Sun, Z.-F. Yao, Y. Lu, X.-Y. Wang, J.-Y. Wang and J. Pei, *Angew. Chem., Int. Ed.*, 2021, **60**, 23313–23319; (*n*) N. Ando, T. Yamada, H. Narita, N. N. Oehlmann, M. Wagner and S. Yamaguchi, *J. Am. Chem. Soc.*, 2021, **143**, 9944–9951; (*o*) L. Fritze, M. Fest, A. Helbig, T. Bischof, I. Krummenacher, H. Braunschweig, M. Finze and H. Helten, *Macromolecules*, 2021, **54**, 7653–7665; (*p*) M. Chen, K. S. Unikela, R. Ramalakshmi, B. Li, C. Darrigan, A. Chrostowska and S.-Y. Liu, *Angew. Chem., Int. Ed.*, 2021, **60**, 1556–1560; (*q*) J.-K. Li, X.-Y. Chen, Y.-L. Guo, X.-C. Wang, A. C.-H. Sue, X.-Y. Cao and X.-Y. Wang, *J. Am. Chem. Soc.*, 2021, **143**, 17958–17963; (*r*) J. Guo, Y. Yang, C. Dou and Y. Wang, *J. Am. Chem. Soc.*, 2021, **143**, 18272–18279; (*s*) Y. Zhang, D. Zhang, T. Huang, A. J. Gillett, Y. Liu, D. Hu, L. Cui, Z. Bin, G. Li, J. Wei and L. Duan, *Angew. Chem., Int. Ed.*, 2021, **60**, 20498–20503; (*t*) S. Oda, B. Kawakami, Y. Yamasaki, R. Matsumoto, M. Yoshioka, D. Fukushima, S. Nakatsuka and T. Hatakeyama, *J. Am. Chem. Soc.*, 2022, **144**, 106–112; (*u*) Q. Zhu, S. Wang and P. Chen, *Org. Lett.*, 2019, **21**, 4025–4029; (*v*) J.-F. Chen, X. Yin, B. Wang, K. Zhang, G. Meng, S. Zhang, Y. Shi, N. Wang, S. Wang and P. Chen, *Angew. Chem., Int. Ed.*, 2020, **59**, 11267–11272; (*w*) G. Ji, N. Wang, X. Yin and P. Chen, *Org. Lett.*, 2020, **22**, 5758–5762; (*x*) C. Li, Y. Shi, P. Li, N. Zhang, N. Wang, X. Yin and P. Chen, *Org. Lett.*, 2021, **23**, 7123–7128; (*y*) F. Zhao, J. Zhao, Y. Wang, H.-T. Liu, Q. Shang, N. Wang, X. Yin, X. Zheng and P. Chen, *Dalton Trans.*, 2022, **51**, 6226–6234; (*z*) X. Tian, J. Guo, W. Sun, L. Yuan, C. Dou and Y. Wang, *Chem.–Eur. J.*, 2022, **28**, e202200045.

9 P. Li, D. Shimoyama, N. Zhang, Y. Jia, G. Hu, C. Li, X. Yin, N. Wang, F. Jäkle and P. Chen, *Angew. Chem., Int. Ed.*, 2022, **61**, e202200612.

10 (*a*) H.-T. Feng, Y.-X. Yuan, J.-B. Xiong, Y.-S. Zheng and B. Z. Tang, *Chem. Soc. Rev.*, 2018, **47**, 7452–7476; (*b*) J. Yu, C. Tang, X. Gu, X. Zheng, Z.-Q. Yu, Z. He, X.-G. Li and B. Z. Tang, *Chem. Commun.*, 2020, **56**, 3911–3914; (*c*) X. Zhang, H. Liu, G. Zhuang, S. Yang and P. Du, *Nat. Commun.*, 2022, **13**, 3543.

11 G. Wang, E. Dmitrieva, B. Kohn, U. Scheler, Y. Liu, V. Tkachova, L. Yang, Y. Fu, J. Ma, P. Zhang, F. Wang, J. Ge and X. Feng, *Angew. Chem., Int. Ed.*, 2022, **61**, e202116194.

12 (*a*) J. Luo, Z. Xie, J. W. Y. Lam, L. Cheng, H. Chen, C. Qiu, H. S. Kwok, X. Zhan, Y. Liu, D. Zhu and B. Z. Tang, *Chem. Commun.*, 2001, 1740–1741; (*b*) J. Mei, N. L. C. Leung, R. T. K. Kwok, J. W. Y. Lam and B. Z. Tang, *Chem. Rev.*, 2015, **115**, 11718–11940; (*c*) Y. Hong, J. W. Y. Lam and B. Z. Tang, *Chem. Soc. Rev.*, 2011, **40**, 5361–5388; (*d*) R. Hu, E. Lager, A. Aguilar-Aguilar, J. Liu, J. W. Y. Lam, H. H. Y. Sung, I. D. Williams, Y. Zhong, K. S. Wong, E. Peña-Cabrera and B. Z. Tang, *J. Phys. Chem. C*, 2009, **113**, 15845–15853.

13 (*a*) W.-M. Wan, D. Tian, Y.-N. Jing, X.-Y. Zhang, W. Wu, H. Ren and H.-L. Bao, *Angew. Chem., Int. Ed.*, 2018, **57**, 15510–15516; (*b*) H. Huang, L. Liu, J. Wang, Y. Zhou, H. Hu, X. Ye, G. Liu, Z. Xu, H. Xu, W. Yang, Y. Wang, Y. Peng, P. Yang, J. Sun, P. Yan, X. Cao and B. Z. Tang, *Chem. Sci.*, 2022, **13**, 3129–3139; (*c*) P. Li, Y. Jia, S. Zhang, J. Di, N. Zhang and P. Chen, *Inorg. Chem.*, 2022, **61**, 3951–3958.